COVER SHEET

TWO-DIMENSIONALLY LOCALIZED MODES OF A NANO-SCALE GAP PLASMON WAVEGUIDE

D. F. P. Pile and T. Ogawa

Department of Optical Science and Technology, Faculty of Engineering, The University of Tokushima, Minamijosanjima 2-1, Tokushima 770-8506, Japan

D. K. Gramotnev

Applied Optics Program, School of Physical and Chemical Sciences, Queensland University of Technology, GPO Box 2434, Brisbane, QLD 4001, Australia

Y. Matsuzaki

Department of Optical Science and Technology, Faculty of Engineering, The University of Tokushima, Minamijosanjima 2-1, Tokushima 770-8506, Japan

K. C. Vernon

Applied Optics Program, School of Physical and Chemical Sciences, Queensland University of Technology, GPO Box 2434, Brisbane, QLD 4001, Australia

K. Yamaguchi, T. Okamoto, M. Haraguchi, M. Fukui

Department of Optical Science and Technology, Faculty of Engineering, The University of Tokushima, Minamijosanjima 2-1, Tokushima 770-8506, Japan

ABSTRACT

We report numerical analysis and experimental observation of two-dimensionally localized plasmonic modes guided by a nano-gap in a thin metal film. Dispersion, dissipation and field structure of these modes are analyzed using the finite-difference time-domain algorithm. The experimental observation is conducted by the end-fire excitation of the proposed gap plasmon waveguides and detection of the generated modes using their edge scattering and CCD camera imaging. Physical interpretation of the obtained results is presented and origins of the described modes are discussed.

Use of plasmons in guiding metallic nano-structures is one of the most promising approaches to overcome the diffraction limit of light [1-3] and significantly increase levels of integration and miniaturization of integrated optical devices and components. Such structures include metal nano-strips [4-6], nano-rods [3, 7], nano-chains [1, 2, 8], wedges [9-11], grooves [12-16], etc. For example, plasmonic waveguides made in the form of a metallic V-groove are characterised by a unique combination of strong sub-wavelength localization and relatively low dissipation [13, 14], single-mode operation [14], possibility of nearly 100% transmission through sharp bends [15], and high tolerance to structural imperfections [16]. As a result, such grooves seem to be one of the best options so far for sub-wavelength waveguiding [13-16], which may eventually lead to the replacement of the current electronic integrated circuits by their more effective all-optical counterparts.

Another type of strongly localized plasmons, that may be as interesting, are plasmons in narrow metallic gaps filled completely or partially with dielectric [17-21]. These plasmons may have especially strong localization in the direction perpendicular to the gap [17-21]. It is also possible to expect that they may experience high transmission through sharp bends, because leakage bend losses into the metal are not possible. Due to the same reason, gap plasmons are expected to be tolerant to structural imperfections, similar to CPP modes in sharp V-grooves [16]. In addition, fabrication of gap plasmon waveguides (GPWs) may be simpler than that of V-grooves.

However, previous attempts to investigate GPWs [17-21] have not resulted in the identification and analysis of dispersion, dissipation, and field structure of specific plasmon modes in gaps of finite dimensions. It is not known if GPWs can support one or more modes, and what are their physical origins. At the same time, this knowledge

will be essential for the correct and optimal design of such sub-wavelength waveguides and their successful application in nano-optics circuits.

Therefore, the aim of this letter is in numerical analysis of plasmonic modes in sub-wavelength waveguides in the form of a nano-gap in a metallic film or membrane (Fig. 1a), and their experimental observation by means of direct excitation using bulk optical waves.

The numerical analysis is carried out by means of the 3-dimensional (3D) finite-difference time-domain (FDTD) algorithm that was previously developed and used for the analysis of groove and wedge plasmons [11,13-16], and the compact-2D FDTD approach [11,22]. The compact-2D FDTD algorithm provides more accurate field distributions and wave vectors [11,22]. However, it cannot be used for irregular guides, e.g., with the end-fire excitation, in which case 3D FDTD has been used.

A GPW of width w in a silver film of thickness h in vacuum or in a uniform dielectric is shown in Fig.1a. GPW modes are generated by the end-fire excitation using a source that has non-zero z-component of the electric field within the aperture matching the cross-section of the gap, placed near the end of the gap at $x = 0$ (Fig. 1a).

As a result, a periodically changing, strongly localized field is generated along the gap – Figs. 1b,c (the structural parameters are presented in the figure caption). In the absence of dissipation, this field is non-decaying along the gap (Fig. 1b). Therefore, it represents a strongly localized plasmonic eigenmode of the GPW. Fourier analysis of the field along the x-axis [13,14] demonstrates that there is only one (fundamental) GPW mode generated in the considered structure. The region of localization of this mode is ~ 140 nm in the y-direction (Fig. 1c), and ~ 40 nm in the z-direction. In planar technology, localization in the plane of the surface is more important for high degree of integration, and this is the case for the GPW mode (Fig. 1b).

Introducing dissipation results in decaying amplitude along the x-axis – Fig. 1c. The propagation distance for the GPW mode in the structure with $h = w = 25$ nm is ≈ 2.3 μm at the $1/e$ level of the field amplitude or ≈ 1.2 μm for energy (Fig. 1c). Increasing w and h results in increasing propagation distance: ≈ 15 μm, ≈ 18 μm, ≈ 21 μm for $h = w = 100$ nm, $h = 150$ nm and $w = 100$ nm, $h = 200$ nm and $w = 100$ nm, respectively. These propagation distances are sufficient for the design of effective sub-wavelength waveguides and interconnectors in integrated nano-optics [1,6,9].

The field structure of the GPW modes has been obtained by the compact-2D FDTD algorithm [11,22]. The electric field distribution in the fundamental GPW mode in the Ag-vacuum structure with $w = h = 100$ nm is presented in Fig. 2a. If w is reduced and h is increased, the gap may eventually support more than one mode. Fig. 2b is typical for the two modes in the GPW, though the pattern may change with x due to beats between the modes. The Fourier analysis [13,14,22] gives the wave numbers $q_{1,2}$ of the fundamental and second modes as functions of h – Fig. 2c.

The most interesting aspect of Fig. 2c is that q_1 and q_2 lie on different sides of the line representing the wave number of the gap plasmon q_{gp} (solid line, $h = \infty$). It can be seen that if h increases, then $q_2 \to q_{gp}$ (circles in Fig. 2c). This is expected, if we assume that the second GPW mode is represented by a gap plasmon with the wave vector $\mathbf{q}_{gp}$, successively reflecting from the edges of the gap at $y = \pm h/2$ (q_2 is the x-component of $\mathbf{q}_{gp}$). This is very similar to how a bulk wave forms a guided slab mode [23]. Increasing thickness of the metal film with the gap is thus similar to increasing thickness of a guiding slab, and this leads to increasing effective dielectric permittivity for guided modes (for the second GPW mode). This is the reason for increasing q_2 with increasing h (Fig. 2c). On the other hand, at $h \lesssim 700$ nm, q_2 is smaller than the wave

number of the surface plasmon (dashed curve in Fig. 2c), and the second GPW mode becomes a leaky mode. At $h \lesssim 600$ nm it also leaks into bulk waves in vacuum (Fig. 2c).

On the contrary, for the fundamental GPW mode $q_1 > q_{gp}$ even if $h \to +\infty$, and $q_1 \to +\infty$ when $h \to 0$ (crosses in Fig. 2c). Therefore, the fundamental GPW mode is related not to gap plasmons, but rather to coupled wedge plasmons [11] propagating along the four corners of the gap (see also Fig. 2a with maximums of the electric field near these corners). If $h \to +\infty$, the two wedge plasmons at $y = h/2$ become uncoupled with those at $y = -h/2$, and we have two identical modes, each formed by just two wedge plasmons coupled across the gap. This is the reason why the wave number of the fundamental GPW mode $q_1 > q_{gp}$ at $h \to +\infty$ (Fig. 2c). In the other limit of $h \to 0$, coupling of the wedge plasmons across the film becomes much stronger than across the gap, because the penetration depth of the plasmons into the gap becomes smaller than the gap width. We get two separate pairs of coupled plasmons – one pair on each side of the gap at $z = \pm w/2$. Thus, when $h \to 0$, the asymptotic behavior of q_1 corresponds to the two coupled wedge plasmons at the rectangular edge of the film (Fig. 2c).

The experimental observation of the GPW modes was achieved in the structure shown in Fig. 3a. An ~ 2.2 μm silver film was evaporated onto a glass substrate. Five ridges of approximately rectangular profile and different widths were etched in the film by means of focused ion beam lithography (FIB), so that the metal was completely removed from the valley regions. A thin Ag film was evaporated onto the structure, so that to cover the valley regions by ~ 100 nm of silver (Fig. 3a). In the three ridges of thicknesses (1) 800 nm, (2) 1200 nm, and (3) 1300 nm, gaps of different widths were etched by means of FIB down to the glass substrate (three gaps in each of the ridges) – Fig. 3a. Typically, gap widths increased up the ridges. The width of the gap in the (*c*-*c*) cross-section (Fig. 3a) varied from $w_1 \approx 70$ nm at the Ag-glass interface to $w_2 \approx 150$ nm

at the top of the ridge. For the gaps in the (*b*-*b*) cross-section: $w_1 \approx 200$ nm, $w_2 \approx 300$ nm.

The structure was illuminated through the glass substrate by a bulk wave with the magnetic field along the *y*-axis, and GPW modes were generated through the holes corresponding to each of the gaps in the ridges. These modes travel up the gaps and scatter into bulk waves at the termination of GPWs at the tops of the ridges. The scattered waves were detected by a CCD camera. The Ag film of ~ 100 nm in the valley regions effectively separated the incident wave and weak scattered signals.

The distribution of the field intensity in the (*b*-*b*) cross-section of the ridges (Fig. 3a), obtained by the CCD camera, is presented in Fig. 3b (solid curve). Maximums of the scattered signals correspond to termination scattering of GPW modes. The dashed curves represent the theoretical intensity distributions in the gaps of $w = w_2 = 300$ nm for the second GPW mode in ridges of (2) $h = 1200$ nm and (3) $h = 1300$ nm. These dependencies have been normalized so that their maximums coincide with the maximums of the experimental dependencies from the CCD camera (Fig. 3b). The agreement between the theoretical and experimental curves (Fig. 3b) suggests that the fundamental mode may not be effectively generated in these GPWs, possibly due to the geometry of the nano-holes at the Ag-glass interface and/or roundness of the gap corners (with the estimated radius of ~ 50 nm). There is no theoretical curve for the first GPW in Fig. 3b, because in this case the second mode is leaky, and no theoretical steady-state distribution of intensity can be obtained. This might also be the reason for maximum 1 in Fig. 3b to be significantly lower than the other two.

At the same time, the measured field intensity in the (*c*-*c*) cross section (Fig. 3a) is significantly different and displays three distinct maximums (solid curve in Fig. 3c). This pattern is typical for interference between the fundamental and second GPW

modes (see Fig. 2b and dashed curve in Fig. 3c). This is an indication that for this gap both the modes are generated (possibly due to less roundness of the gap corners).

Note that if the polarization of the incident laser beam is such that the magnetic field is along the *z*-axis, no scattered waves from the termination of GPWs have been observed. In addition, the widths of the maximums of the measured intensity (Figs. 3b,c) are smaller than the *y*-dimensions of the nano-holes through which excitation of the GPW modes occurred. These are additional confirmations that we have indeed observed GPW modes, rather than simple transmission through the nano-apertures.

Thus, this paper has reported the numerical analysis and the first experimental observation of a new type of strongly localized plasmon modes guided by a rectangular gap in a thin metal film/membrane. These plasmon modes may be one of the best options for the design of all-optical nano-circuits and devices, mainly because of their significant propagation distance, very strong localization, expected low bend losses (compare with [15]), relatively simple fabrication of the required structures, etc.

The authors gratefully acknowledge support from the Japan Society for the Promotion of Science and the High Performance Computing Division at the Queensland University of Technology as well as valuable assistance given by Kenzou Yamaguchi.

Since the submission of this manuscript a paper that numerically treats a similar problem was published [24].

References

1. J. R. Krenn, Nature Mater. **2**, 210 (2003).
2. S. A. Maier, P. G. Kik, H. A. Atwater, S. Meltzer, E. Harel, B. E. Koel, and A. A. G. Requicha, Nature Mater. **2**, 229 (2003).
3. J. Takahara, S. Yamagishi, H. Taki, A. Morimoto, and T. Kobayashi, Opt. Lett. **22**, 475 (1997).
4. P. Berini, Phys. Rev. B. **63**, 125417 (2001); G. Schider, J. R. Krenn, A. Hohenau, H. Ditlbacher, A. Leitner, F. R. Aussenegg, W. L. Schaich, I. Puscasu, B. Monacelli, and G. Boreman, Phys. Rev. B. **68**, 155427 (2003).
5. B. Lamprecht, J. R. Krenn, G. Schider, H. Ditlbacher, M. Salerno, N. Felidj, A. Leitner, and F. R. Aussenegg, Appl. Phys. Lett. **79**, 51 (2001).
6. J. R. Krenn, B. Lamprecht, H. Ditlbacher, G. Schider, M. Salerno, A. Leitner, and F. R. Aussenegg, Europhys. Lett. **60**, 663 (2002).
7. C. A. Pfeiffer, E. N. Economou, and K. L. Ngai, Phys. Rev. B. **10**, 3038 (1974).
8. J. R. Krenn, A. Dereux, J. C. Weeber, E. Bourillot, Y. Lcaroute, J. P. Goudonnet, G. Schider, W. Gotschy, A. Leitner, F. R. Aussenegg, and C. Girard, Phys. Rev. Lett. **82**, 2590 (1999); S. A. Maier, M. L. Brongersma, and H. A. Atwater, Appl. Phys. Lett. **78**, 16 (2001).
9. T. Yatsui, M. Kourogi, and M. Ohtsu, Appl. Phys. Lett. **79**, 4583 (2001).
10. A. D. Boardman, G. C. Aers, and R. Teshima, Phys. Rev. B. **24**, 5703 (1981).
11. D. F. P. Pile, T. Ogawa, D. K. Gramotnev, T. Okamoto, M. Haraguchi, M. Fukui, and S. Matsuo, Appl. Phys. Lett, (accepted).
12. I. V. Novikov and A. A. Maradudin, Phys. Rev. B. **66**, 035403 (2002).
13. D. F. P. Pile and D. K. Gramotnev, Opt. Lett. **29**, 1069 (2004).
14. D. K. Gramotnev and D. F. P. Pile, Appl. Phys. Lett. **85**, 6323 (2004).

15. D. F. P. Pile and D. K. Gramotnev, Opt. Lett., **30**, 1186 (2005).

16. D. F. P. Pile and D. K. Gramotnev, Appl. Phys. Lett., **86**, 161101 (2005).

17. K. Tananka and M. Tanaka, Appl. Phys. Lett. **82**, 1158 (2003).

18. K. Tananka, M. Tanaka, and T. Sugiyama, Optics Express. **13**, 256 (2005).

19. B. Wang and G.P. Wang, Appl. Phys. Lett. **85**, 3599 (2004).

20. B. Wang and G.P. Wang, Opt. Lett. **29**, 1992 (2004).

21. F. Kusunoki, T. Yotsuya, J. Takahara and T. Kobayashi, Appl. Phys Lett. **86**, 211101 (2005).

22. D. F. P. Pile, Appl. Phys. B, **81**, 607-613 (2005).

23. A. Yariv, P. Yeh, Optical Waves in Crystals: Propagation and Control of Laser Radiation. J. Wiley & Sons, New York (1984).

24. L. Liu, Z. Han and S. He, Optics Express, **13**, 6645 (2005).

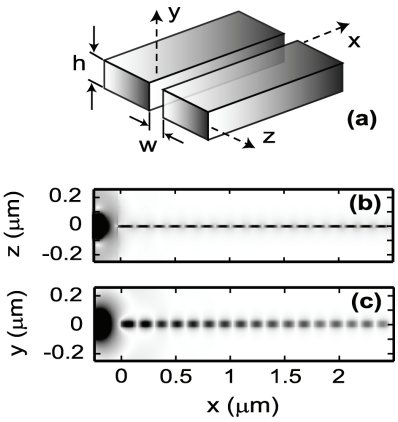

Fig.1. (a) GPW in the form of a rectangular gap of width w in a metal film/membrane of thickness h. The origin of the frame coincides with the central point of the gap in the (y,z) plane. (b) The FDTD distribution of the magnitude of the electric field $|E|$ (arbitrary units) in the (x,z) plane for the following parameters: $h = w = 25$ nm, $\lambda_{vacuum} = 632.8$ nm (He-Ne laser), permittivity of the metal is real: $\varepsilon_m = -16.22$ (silver with no dissipation), the metal membrane is in vacuum ($\varepsilon_d = 1$). (c) Same as for (b) but in the (x,y) plane and in the presence of dissipation: $\varepsilon_m = -16.22 + 0.52i$.

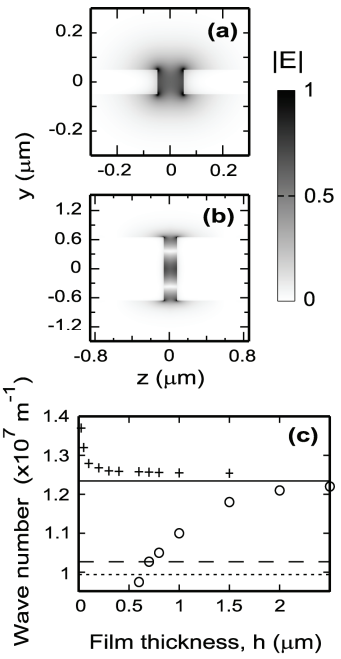

Fig. 2. (a) The (y,z) distribution of the magnitude of the electric field (compact-2D FDTD [11,22], in arbitrary units) in the fundamental GPW mode in the silver-vacuum structure with $w = h = 100$ nm ($\lambda_{vacuum} = 632.8$ nm, $\varepsilon_m = -16.22 + 0.52i$). (b) The typical ($y$,$z$) distribution of the electric field resulting from interference (beats) between the fundamental and second GPW modes in the silver-vacuum structure with $w = 150$ nm and $h = 1300$ nm ($\lambda_{vacuum} = 632.8$ nm, $\varepsilon_m = -16.22 + 0.52i$). (c) The dependencies of the wave numbers of the fundamental (crosses) and second (circles) GPW modes on thickness of the silver film at $w = 100$ nm. Solid line: wave number of symmetric (with respect to magnetic field) gap plasmons in the infinite silver-vacuum gap of $w = 100$ nm. Dashed line: wave number of surface plasmons on an isolated smooth silver-vacuum interface. Dotted line: wave number in vacuum ($\lambda_{vacuum} = 632.8$ nm).

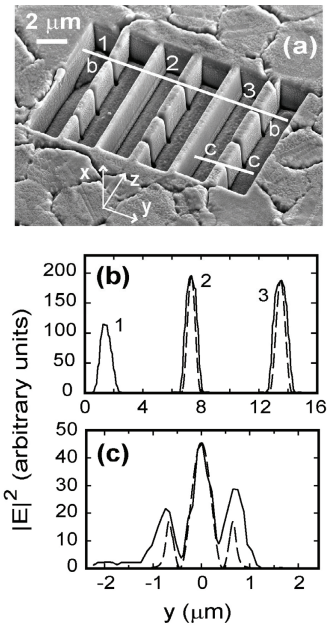

Fig. 3. (a) The SEM image of the experimental structure with five silver ridges of height ≈ 2.2 μm on the glass substrate. The thickness of the silver film in the valley regions is ~ 100 nm. Three ridges (membranes) of thicknesses (1) $h \approx 800$ nm, (2) $h \approx 1200$ nm, and (3) $h \approx 1300$ nm contain gaps etched down to the glass substrate. Widths of the gaps in the (*b*-*b*) cross-section: at the top of the ridge $w_2 \approx 300$ nm, at the bottom of the ridge $w_1 \approx 200$ nm, and in the (*c*-*c*) cross-section: $w_2 \approx 150$ nm, $w_1 \approx 70$ nm. A laser beam is incident onto the structure from underneath through the glass substrate. The signals from scattering of the generated GPW modes at the gap terminations at the tops of the ridges is registered by a CCD camera. (b) The experimental distribution of the signal intensity on the CCD camera (solid curves), and the corresponding theoretical curves (compact-2D FDTD) of the intensity distribution in the second GPW mode with $w = w_2$ and the corresponding thicknesses of the ridge/membrane. (c) Same as (b), but for the gap in the (*c*-*c*) cross-section with $w = w_2 \approx 150$ nm. The dashed theoretical curve represents the typical intensity distribution for a beat between the fundamental and second GPW modes (Fig. 2b).